



Experimental studies of spheromak formation

H. Bruhns, C. ChinFatt, Y. P. Chong, A. W. DeSilva, G. C. Goldenbaum, H. R. Griem, G. W. Hart, R. A. Hess, J. H. Irby, and R. S. Shaw

Citation: [Physics of Fluids \(1958-1988\)](#) **26**, 1616 (1983); doi: 10.1063/1.864297

View online: <http://dx.doi.org/10.1063/1.864297>

View Table of Contents: <http://scitation.aip.org/content/aip/journal/pof1/26/6?ver=pdfcov>

Published by the [AIP Publishing](#)

Articles you may be interested in

[Spheromak formation and sustainment studies at the sustained spheromak physics experiment using high-speed imaging and magnetic diagnostics](#)

Phys. Plasmas **13**, 022502 (2006); 10.1063/1.2140682

[Scaling studies of spheromak formation and equilibrium](#)

Phys. Plasmas **5**, 1027 (1998); 10.1063/1.872632

[Experimental study of a transformerdriven spheromak plasma](#)

Phys. Fluids B **3**, 2591 (1991); 10.1063/1.859971

[Experimental study of the relaxation cycle of a decaying spheromak in an external magnetic field](#)

Phys. Fluids B **3**, 1452 (1991); 10.1063/1.859711

[Formation of a flux core spheromak](#)

Phys. Fluids B **3**, 1041 (1991); 10.1063/1.859832



AIP | Journal of
Applied Physics

Journal of Applied Physics is pleased to
announce **André Anders** as its new Editor-in-Chief

Experimental studies of spheromak formation

H. Bruhns,^{a)} C. Chin-Fatt, Y. P. Chong,^{b)} A. W. DeSilva, G. C. Goldenbaum,
H. R. Griem, G. W. Hart, R. A. Hess, J. H. Irby,^{c)} and R. S. Shaw

Laboratory for Plasma and Fusion Energy Studies, University of Maryland, College Park, Maryland 20742

(Received 27 May 1982; accepted 10 February 1983)

Studies in the PS-1 spheromak experiment show that a spheromak configuration can be effectively formed by a combined z - and θ -pinch technique on both a fast ($\tau_{\text{formation}} \simeq \tau_{\text{Alfvén}}$) and a much slower timescale. The gross tilt and shift instability of the toroid can be suppressed by a combination of conducting walls, shaping the separatrix by externally applied fields, and the use of "figure-eight" coils. Optimum stability is obtained for almost spherical toroids. Maximum field-reversal times for stable, well-confined toroids are $\geq 40 \mu\text{sec}$, consistent with resistive decay. Temperatures during the stable decay are 5–10 eV; impurity radiation is an important energy-loss mechanism.

I. INTRODUCTION

The spheromak, a toroidal-plasma configuration confined by poloidal and internally generated toroidal magnetic fields, has recently attracted much theoretical and experimental interest, mainly for two reasons. First, a spheromak fusion reactor would allow operation with topologically much simpler blanket and coil structures than would a tokamak, because it does not require a conducting wall or coil linkage through the center of the torus. In a way, it combines the favorable topological features of open field line devices, such as mirrors, with some of the plasma-confinement advantages of closed field line devices. Second, since a considerable part of the magnetic pressure necessary to balance the pressure of the plasma and the internal magnetic field is produced by plasma currents, the expected engineering beta value (referred to the magnetic field at the coil location) is large compared to that in tokamaks. This leads to considerably relaxed structural requirements for coil support in a reactor scale device and to a significant reduction in the cost of the confinement coils and their driving power source, possibly eliminating the need for superconducting coils.

The physics of the spheromak concept has only recently begun to be thoroughly investigated. Taylor,¹ following previous work by Woltjer and others,² predicted a relaxation to a force-free minimum energy state for reversed-field configurations which keeps the magnetic helicity globally invariant. The loss processes involved in this relaxation were not specified. Although the details of this relaxation may affect the ratio of initial to final field energy, as well as the plasma density and impurity levels, the resulting force-free equilibrium can be described without knowledge of the way it was established. Force-free magnetic configurations have been previously investigated in the transformer-driven reversed-

field-pinch experiments.³ This equilibrium has been investigated theoretically for spheromaks in both spherical and cylindrical configurations using Taylor's method.⁴ There is now sufficient experimental evidence from the coaxial gun-produced spheromaks,⁵ conical theta-pinch-produced spheromaks,⁶ from the Princeton slow-formation Proto S-1 experiment,⁷ and from the Maryland pinch-produced PS-1 spheromak⁸ that the magnetic field profiles correspond reasonably well to force-free equilibria. This is not surprising since the temperatures are low at present, so that the plasma pressure can be neglected. Exceptions are those experiments in PS-1 having strong radial compression of the toroid, where large-beta values are obtained.

The stability of the confined plasma-magnetic field structure is a major concern. Theoretical studies show that the most dangerous magnetohydrodynamic (MHD) mode is the $m = 1$ tilt/shift instability.^{4,9} The tilt mode, which is not observed in field-reversed theta pinches,¹⁰ appears in spheromaks of prolate shape,^{4,11} while the shift mode appears in more spherical and oblate ones.¹² Generally, it is believed that wall stabilization is required to suppress these modes.^{4,13} This could be a considerable liability for a spheromak reactor if the separatrix everywhere is in contact with a wall.¹⁴ It is therefore of interest to study the stability of a spheromak which is not completely surrounded by a conduction shell. The spheromak obtained in the PS-1 experiment at the University of Maryland using dielectric walls has been studied in detail. The basics of this experiment and the method of formation are described elsewhere.^{8,12} First results showed that a toroid was formed and was stable up to 30 μsec after formation judging from axially line-integrated interferometry.⁸ However, when magnetic-probe measurements were performed, a tilt of the toroid appeared shortly after complete field reversal. The shape of the toroid was very prolate. In accordance with theory, making the plasma oblate at the expense of radial compression eventually resulted in a stable configuration.^{11,12}

Here we report on the equilibrium, stability, and plasma parameters of the PS-1 spheromak in several experimen-

^{a)} Permanent address: Institut für Angewandte Physik II, Universität Heidelberg, Albert Uberle Str. 3–5, D6900 Heidelberg, Germany.

^{b)} Present address: Lawrence Livermore National Laboratory, Livermore, California 94550.

^{c)} Present address: Massachusetts Institute of Technology, Cambridge, Massachusetts 01003.

tal configurations which allowed for variations of the shape of the toroid from very prolate to very oblate, as well as for variation of the external magnetic field. After discussing the diagnostics in Sec. II, we describe, in Sec. III, experiments with a fast-formation scheme, using a full theta-pinch coil, a split coil, and a more complicated double-coil structure, producing constant or even rising external fields during the confinement phase. In Sec. IV, we present experiments using slow external field reversal, which is of interest for the creation of larger spheromaks where fast-formation techniques become impractical. The formation time scale in these experiments is comparable to that of the Princeton experiment⁷ (which, however, employs a rather different technique to create the field).

In Sec. V, we will discuss the results of introducing a thin metallic liner inside the dielectric vacuum wall, which decreased the axial current through the toroid as well as enhanced stability and reduced impurities. Finally, the effects of Ioffe currents and “figure-eight” coils on stability are also described in Sec. V.

II. DIAGNOSTICS

Information on lifetime, shape, equilibrium-field magnitudes, and stability of the toroidal configuration was obtained from magnetic-field measurements. Internal fields have been measured using three different types of magnetic probes. The first two cases in the following section were diagnosed using an L-shaped probe (probe 1) which simultaneously measured the axial (B_z) and toroidal (B_ϕ) components of the field for one spatial position. The remaining measurements in Sec. III were performed using a straight probe (probe 2) which measured B_z , B_ϕ , and B_r simultaneously at two spatial positions separated axially by 8 cm. Scans were obtained on a discharge-to-discharge basis by varying the position of the probe. To reduce the number of discharges necessary for a magnetic-field scan and to ensure better radial correlation between the signals at different positions, a different probe setup has been utilized for the remaining cases discussed in Secs. IV and V. This probe (3) consisted of two L-type probes which enabled all three components of the magnetic field vector to be measured simultaneously at ten different positions $r = 1, 3, 5, 7,$ and 9 cm and $\phi = 0$ and π . All these probes entered the discharge tube parallel to the axis. Probes 3 were supported by booms near the wall at $r = 10$ cm, and the active portion containing the coils protruded radially from the sides into the center of the device. Radial profiles at different axial positions of the toroid were measured by sliding the probes parallel to the z axis. All the probes were isolated from the plasma by a glass casing and had an internal copper shield to reduce pickup. The signals were passively integrated with a time constant of $500 \mu\text{sec}$ and then processed by fast 8 bit analog-digital converters (LeCroy 2256). Due to the limited number of converters available, only 15 of the total of 30 signals could be recorded on each discharge. All probes have been calibrated with a Helmholtz coil at frequencies of 0.01 – 10 MHz. Magnetic pickup due to misorientation of the coils was determined from vacuum discharges generally found to be negligibly small. Electrical pickup has been determined to be negligible

by rotating the probes. The effect of the probes on the plasma has been investigated by simultaneously inserting probes 2 and 3. Signals were recorded on plasma shots alternatively retracting one of the probes axially. We concluded that the L-type probe affects the plasma less than the straight one. The latter caused a larger reduction of field-reversal time, as well as a stronger tendency for the toroid to be destroyed by a tilt-shift instability.

Provisions were made to measure the total flux enclosed by the cylindrical container at three axial positions: in the symmetry plane and in two other locations which could be varied between $z = 2$ – 8 cm. The axial field strength at the wall outside the chamber was recorded by a passively integrated magnetic pickup probe. Attempts were made to determine a shift of the plasma and possibly also a tilt with a set of three external coils. However, in only a very few cases was an unambiguous interpretation of the signals possible. The currents from the (up to five) capacitor banks were monitored by Rogowski loops.

Plasma densities have been obtained from 6328 \AA He–Ne interferometry operating in quadrature mode with the beam traversing the axial length of the device twice. Radial scans were performed from $r = 0$ – 7 cm and $\phi = 0, 180^\circ$. Fringes were, in general, easily detected except near the axis where no clear interpretation of the two orthogonal channels could be achieved at early times. Additional information on the density behavior was obtained from spectroscopic measurements of the Stark broadening of $D_{\beta,\gamma}$ and He II 3203 \AA (10% helium was added to the D_2 fill for helium line measurements). Emission spectroscopy measurements were performed with a conventional $1/2$ m spectrometer both radially and axially while an optical multichannel analyzer viewed the plasma in the axial direction to provide radial resolution. Relative electron density measurements were derived from the intensity of 90° Thomson scattering using a ruby laser. The electron temperature was determined using this diagnostic for two configurations; in the others, it was inferred from spectroscopic data. Ion temperatures were estimated from time-resolved measurements of the Doppler broadening of C III 2297 \AA and He II 4686 \AA . Impurity radiation has been photographically measured axially with a normal incidence vacuum ultraviolet spectrometer, which was scanned between 450 \AA and 2400 \AA to obtain the total emitted power. Absolute calibration of the instrument was performed by the branching ratio technique. The development of the luminous plasma structure was observed with a single discharge framing camera.

III. EXPERIMENTS WITH FAST FORMATION

The original experiment relied on the formation technique of field-reversed theta pinches (FRC) by using a fast-reversal bank.⁸ A problem in FRC experiments is the poor trapping of bias flux. However, the annular axial current discharge, which occurs in PS-1 immediately before firing the reversal bank, was found to provide an effective trapping of the internal axial flux. In addition, the nominally axial current discharge excites a paramagnetic azimuthal current which may even lead to a poloidal-flux enhancement. In most of the cases discussed in this paper, the magnitude of

the trapped poloidal flux at the time of X-point formation is more than 70% of the initial bias flux inside the radius of the electrode ring.

A. Full solenoid

Using a full-solenoid theta-pinch coil [Fig. 1(a)] and a reversal bank with a rise time of $1.7 \mu\text{sec}$, the formation of a toroid was achieved in approximately $2.5 \mu\text{sec}$ which is 1–3 radial Alfvén times ($r_{\text{wall}} = 11 \text{ cm}$). The vacuum fields at $r = 0, z = 0$ were 1 kG for the bias and 2.4 kG for the reversal field. The results of these experiments have been reported elsewhere.⁸ The ion temperature obtained (approximately 200 eV) was unlikely to be produced entirely by adiabatic heating alone. However, since the measurements are axially averaged, nonMaxwellian features may have led to some uncertainty in temperature. Formation calculations¹⁵ using a hybrid code predict a maximum ion temperature of 60 eV and show that anomalous energy transfer to the ions must be invoked in the calculation in order to obtain the experimentally observed ion temperature.

After installation of crowbar switches into the capacitor banks, studies of the lifetime and properties of the elongated toroid became possible. Axial interferometry showed an annular shape of the plasma to be present until $30 \mu\text{sec}$ after formation. This was taken as evidence that the toroid lasted for this period. However, when a magnetic probe was inserted, a tilt was observed to start immediately after formation of the axial X points. Since no external field or flux

measurements had been performed in this case, it was not clear whether the probe itself had caused the tilt. Also, probe and interferometric measurements could not be done simultaneously in the experimental setup used.

While the theoretical analysis of the stability of force-free MHD configurations predicts a tilt instability for elongated structures, the result may not hold for this case. Due to both the high-beta value and the fact that a considerable fraction of axial current and open field lines passed through the separatrix-bounded region, a comparison with theory is difficult. Also, since the ion gyroradius at the observed temperature is only approximately an order of magnitude smaller than the current sheath width, finite-Larmor-radius effects may be important for stability.

B. Mirror coil

In order to obtain a toroid with smaller length-to-radius ratio (L/R), the center part of the theta-pinch coil was removed. Thus a mirror coil was established with a vacuum field mirror ratio of approximately 1.2 on axis [Fig. 1(b)]. The experiment was operated with vacuum fields of 0.8 kG for the bias and 2 kG for the reversal fields at ($z = 0, r = 0$). It was found that a toroid could be generated which lasted for 30–35 μsec and was stable to tilt and shift. This depended very strongly on the amplitude of the axial current and its timing with respect to the reversal bank discharge. Figure 2 shows contours of constant poloidal flux obtained from magnetic data taken with probe 1 at z positions of 0, 5, 10, and 13.5 cm and r positions from 0 to 10 cm at steps of 2 cm in both $\phi = 0, 180^\circ$. Unlike the full coil solenoid experiment, three magnetic islands are initially established and soon merge into two very pronounced ones. Most of the initial confined flux of the outer island is expelled axially beyond $z = 15 \text{ cm}$, while the center torus expands. Note that data have been taken at both positive and negative radii, hence the observed island structure, which shows good axial symmetry, is unlikely to be probe-induced artifact. The separatrix of the toroid formed with this coil arrangement was still slightly prolate and, hence, according to theory should be tilt unstable. However, the structures observed are not identical to the force-free models assumed. In fact, the ratio of the axial-field component near the midplane to that at larger z values near the X point corresponds in the cylindrical force-free model to an almost spherical shape, $L/R \approx 1.8$ – 2.5 . This is the range where optimum stability against tilt or shift instabilities is expected.^{4,16}

Figure 3 shows the maximum amount of poloidal flux inside the separatrix plotted versus time after the start of the I_z circuit. For times when the separatrix extends beyond the field of view, only that portion in view is considered. The initial strong increase in flux relative to the bias flux is due to a poloidal-flux generation. The conversion of toroidal flux into poloidal flux has been discussed by Alfvén¹⁷ and was interpreted in terms of a kink instability. In this case, however, no macroscopic helical structure is seen. Instead, the tendency of the applied axial current to follow the helical field, which is the resultant of its own self-field and the bias magnetic field is believed to be the likely mechanism for the enhancement of poloidal flux.

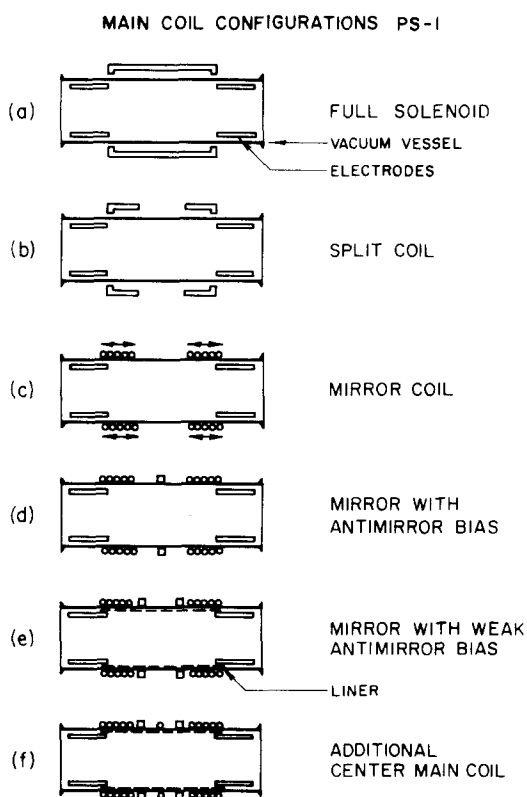


FIG. 1. Major coil configurations of the PS-1 experiment. The diameter of the vessel is 23 cm, the electrode radius 7.8 cm, and the axial distance between the electrodes 30 cm. The capacitor banks are $18 \mu\text{F}$ and 20 kV (bias), $28 \mu\text{F}$ and 20 kV (I_z), and $7.8 \mu\text{F}$ and 40 kV for the main bank in cases (a)–(e) or $28 \mu\text{F}$, and 40 kV in cases (d)–(f).

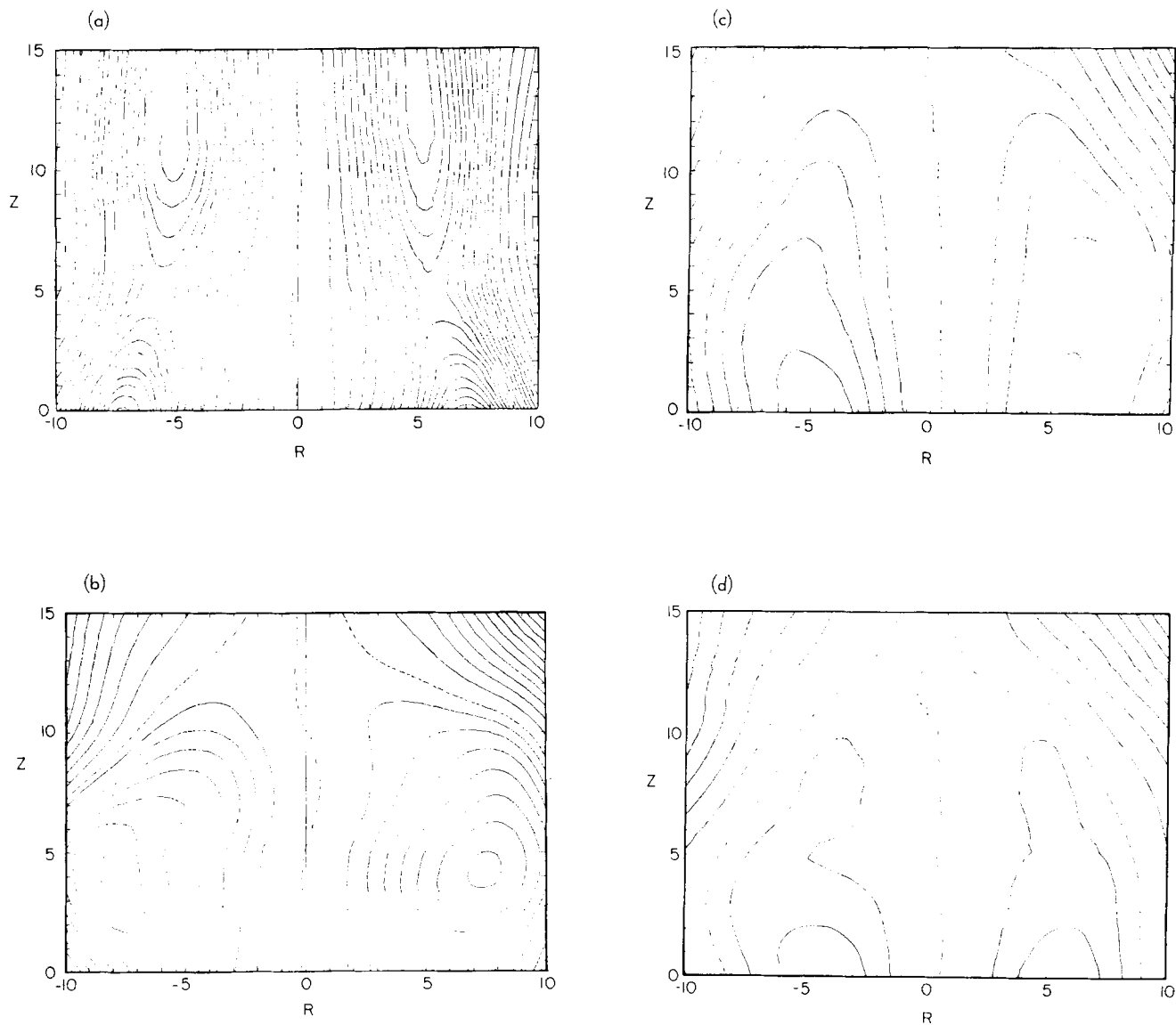


FIG. 2. Contours of constant poloidal flux at different times, for coil configuration 1(b). Inside the separatrix (dashed line) the flux increment is $2\pi \times 5 \text{ kG cm}^2$, outside the increment is $2\pi \times 10 \text{ kG/cm}^2$. (a) $t = 2 \mu\text{sec}$, (b) $t = 8 \mu\text{sec}$, (c) $t = 14 \mu\text{sec}$, and (d) $t = 20 \mu\text{sec}$.

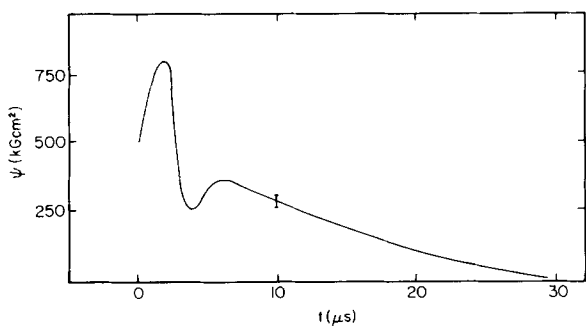


FIG. 3. Poloidal flux versus time in the toroid (i.e., axial flux inside magnetic axis) for coil configuration 1(b). The point at $t = 0$ corresponds to the initial bias flux and the error bars are associated with the contour separations in Fig. 2.

In Fig. 4 we show measured current-density vectors 18 μsec after reversal bank discharge computed from the measured toroidal field. Even at late times, when the poloidal-flux contours look very smooth and regular, a considerable fraction of the total current passes through the center of the toroid by crossing the separatrix predominantly near the X point. A likely reason for this behavior can be found by observing that the poloidal field lines, which are close to the electrode tips at $z = 15 \text{ cm}$, intersect the dielectric wall near the symmetry plane during formation. Hence, the current cannot pass around the outside separatrix without crossing magnetic-field lines. It is therefore favorable for the current to follow the poloidal-field lines close to the X points and to pass through the center of the device. Attempts to reduce this current or to reverse its direction after formation resulted in a somewhat shorter lifetime of the toroid. At present, it

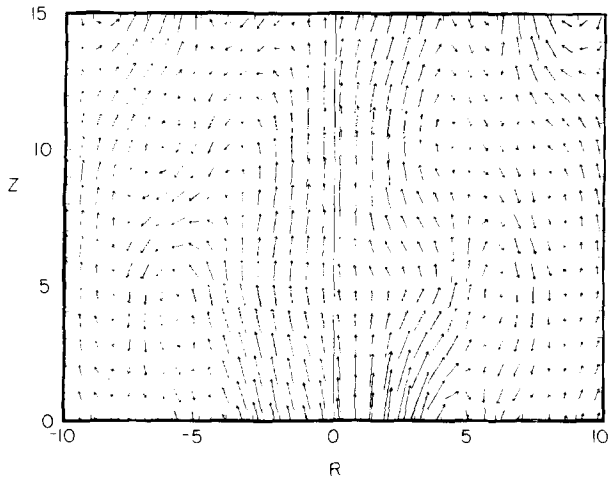


FIG. 4. Current vectors for coil configuration 1(b) at 18 μ sec after reversal bank discharge.

is not possible to rapidly eliminate the external current after formation because of the large inductance of the crowbar circuit.

Figure 5(a) shows the time dependence of the magnetic energy W [$\int (B^2/2\mu)d\tau$], and the helicity K ($\int \mathbf{A}\cdot\mathbf{B}d\tau$) integrated over the separatrix-bounded region, and the eigenvalue k ($= W/K$) for the equilibrium. When the separatrix is outside the wall, the integration is carried out only over the portion visible, also in the fast formation measurements reported here, complete scans for $z < 0$ were not taken and symmetry was invoked based on a sample of measurements. (Later detailed measurements in the slow formation scheme showed symmetry about the $z = 0$ midplane. Here, time zero corresponds to the time of the discharge of the reversal bank.) The strong increase of magnetic energy between 0 and 2 μ sec coincides with the poloidal-flux amplification by the axial current and with the generation of poloidal field by the reversal-field circuit. The following decrease between 2 and 4 μ sec is due to the violent establishment of the toroid, connected both with strong dissipation as well as convective loss of magnetic energy and helicity axially out of the field of view. In the next two microseconds both poloidal flux and magnetic energy increase somewhat, the source again being the axial current.

Typical c III ion temperatures outside the magnetic axis are 40 eV between 2 and 4 μ sec dropping to approximately 20 eV at 5 μ sec and ≤ 10 eV at 20 μ sec. Inside the magnetic axis, peak ion temperatures are > 100 eV at 2–4 μ sec, dropping rapidly to the same values as measured on the outside. Spectroscopic line shapes at $t > 10$ μ sec are generally Gaussian, although for $t < 5$ μ sec, significant Doppler shifts and line splitting exist which indicate directed ion motion and nonthermal features. For this case electron temperatures have not been measured by Thomson scattering. Estimates from observed line excitation indicate T_e approximately 20–30 eV at $t < 5$ μ sec and T_e approximately 5–10 eV at $t > 10$ μ sec. For these late times, therefore, we have equilibration of T_i and T_e .

Impurity radiation between 450 and 2400 \AA (where one expects most of the radiative power to be) was found to con-

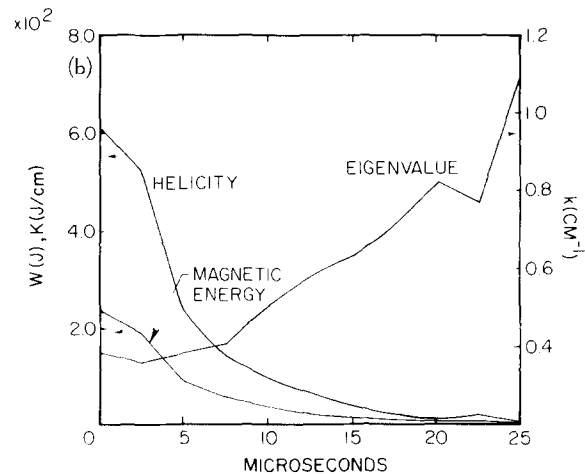
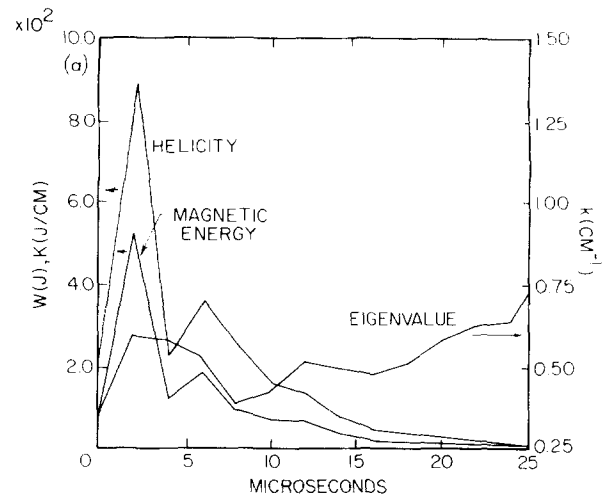


FIG. 5. Magnetic energy W ($\int B^2/2\mu d\tau$), helicity K ($\int \mathbf{A}\cdot\mathbf{B}d\tau$), integrated over the separatrix-bounded region, and eigenvalue k (W/K) of the toroid as function of time. (a) coil configuration 1(b). Note that the flat part of the curve $k(t)$ corresponds to the toroid having almost constant size. (b) coil configuration 1(c) (weak antimirror bias with liner).

tribute only in the 10%–20% range to the total loss in magnetic energy. However, noting the rapid early convective loss of magnetic energy and assuming classical resistivity, radiative loss might account for as much as 50%–100% of the Ohmic power balance except in the very early formation phase where its contribution is less. The main impurities are carbon, oxygen, and nitrogen. The source of carbon is most likely the electrodes, which in this case have graphite tips rather than elkonite tips as were used in the full solenoid experiments.

The field-reversed toroid decayed in 30–35 μ sec. This is also approximately the $1/e$ time of the externally applied field. As a consequence, there is no appreciable radial compression of the toroid with time except for the last five microseconds before loss of field reversal. When a longer-lasting external field was applied, a rapid decay of the toroid by tilting occurred. This is presumably due to the radial compression of the toroid as the internal magnetic field and plasma pressure decreased with respect to the external field. This decay became especially pronounced when a concentric two-coil system was installed with a resistive one-turn coil dri-

ven by the fast capacitor bank and an outer multiturn coil driven by a 10 kV, 380 μF bank having a rise time of 80 μsec . As soon as the decrease of the field produced by the fast bank was overcome by the rise of the slow bank, the plasma started to tilt. An additional problem in this coil system arose from the time-varying external mirror ratio due to the physical separation of the coils and their mutual inductance, which was not negligible compared to the total inductances in the circuits. With this coil arrangement, the plasma toroid was shaped slightly prolate, $L/R \approx 2-2.5$.

IV. EXPERIMENTS WITH SLOW FORMATION—OBLIMAKS

In large experiments, one would face serious difficulties using a fast formation scheme; to maintain short rise times would imply high-voltage energy storage. The PS-1 experiment was therefore redesigned to study slower formation (i.e., of the order of ten Alfvén transit times). Instead of the solid single-turn coil segments used so far, a multiturn coil made with cables was used [Fig. 1(c)]. In addition to increasing the coil inductance, this change allowed a reduction in coil diameter by 10%. With this coil system, a much more efficient use of the available stored energy resulted. Also, by sliding these coils to different axial positions, the mirror ratio could be varied continuously between 1 and 1.5 at vacuum field strengths of 4–7 kG. The rise time of the banks increased to 6.5 μsec and the decay time to 120 μsec . With the fields and densities employed, the formation took 5–15 Alfvén times. On this time scale, the formation proceeded as well as before. Any loss of bias flux was compensated for by the previously mentioned flux enhancement connected with the axial current. However, as was found in previous studies, a tilt or a shift destroyed the plasma 10–20 μsec after field reversal, at which time the torus has shrunk away from the wall. The exact time depends on the shape of the torus.

In order to study even slower formation, experiments were performed using the bias bank only. External field reversal was obtained by crowbarring the capacitors after circuit current reversal, at a time equal to $\frac{3}{4}$ of the period of the circuit. The rise time of the reversal field was then 16 μsec , measured from peak bias to peak reversed field. In this case, it was not possible to achieve sufficient compression to move the separatrix radially inside the wall, since the reversal field was approximately of the same magnitude as the bias field. As a result, long-lasting field reversal was obtained without any gross instabilities. No significant net flux loss occurred initially since the axial current discharge created poloidal flux to compensate the losses. A strong dependence of the lifetime on the duration of the axial current discharge was observed, with most of this current passing through the center of the toroid. Field-reversal times as long as 60 μsec were obtained. Due to the boundary conditions imposed by the separatrix intersecting the walls and the open axial current passing through the region of closed poloidal flux, the equilibrium obtained was quite dissimilar to that of a spheromak. The configuration, however, resembled the one obtained by Alfvén and co-workers in their magnetic-gun experiment, with the plasmoid moving into a chamber with dielectric walls.¹⁸ In their case, the toroid showed excellent

stability and long lifetime.

Attempts were made to compress the toroid radially by enhancing the reversal field until the separatrix was pushed inside the chamber. These attempts resulted in a tilt-shift instability of the torus. Temperatures were lower than before since the magnetic fields as well as their rise times were low. Hence, Ohmic heating was weak, and parallel electron heat conduction to the walls and possibly impurity transport into the plasma were likely candidates for major energy loss.

During these studies, it was observed that even after applying an axial field with a large mirror ratio, the poloidal magnetic topology tended to remain prolate to spherical; no clearly oblate plasmas with the separatrix inside the chamber could be created. In addition, formation of the toroid generally started out with the creation of two axially aligned toroids, located symmetrically about the midplane. These toroids eventually merged. This behavior is believed to be in part due to the mirror-shaped bias field, which allowed the axial current to trap more bias flux near the electrodes than in the midplane. However, as in the case of a full solenoid, the initial stage of field reversal results in double toroids, so that other processes like tearing modes have to be invoked for a complete explanation. Similar multi-island structures have been found in field-reversed theta pinches.¹⁹

The establishment of double or multitoroid configurations might be helpful to the formation of the spheromak. Experimentally, there is some evidence that a tilt or shift instability develops only after the double structure has merged almost completely. A possible explanation is that the total structure is prolate and is predicted theoretically to be stable to the shift. However, each individual toroid is oblate and is predicted to be stable to a tilt. Furthermore, the mutual interaction of the magnetic dipoles of the toroids may tend to stabilize against a tilt. Another aspect is the release of magnetic energy during the merging process of the toroids.²⁰ Theoretically, this energy should be converted into plasma energy and may help to burn through the impurity radiation barrier. However, this possible advantage is connected with lower magnetic fields and currents during the confinement phase and is not seen experimentally at present.

In order to investigate formation without a double toroid phase, the coil system was then equipped with a separate coil for the bias circuit in order to give an antimirror bias-field structure [Fig. 1(d)]. This provided more trapping of bias flux by the axial current near the midplane ($z = 0$) and avoided the double-toroid formation. In addition, the antimirror bias field aided in preventing the axial current from running into the glass walls during the initial phases of the discharge. This should reduce the emission of impurities from the walls. No clear effect was discernible, however.

An additional goal was to get better control of the shape of the toroid by controlling (both during and after the formation) the separatrix position near the midplane by the independent bias circuit, while at the same time applying strong axial compression with the reversal-field mirror coils. A disadvantage of this setup was that the different time constants of the reversal and bias banks did not allow simultaneous field reversal at $z > 5$ cm, where the mirror coils dominated, and $z < 5$ cm, where the bias coil located around the mid-

plane dominated the field shape. Effectively, the experiment had an external double cusp reversal field during formation. Hence, during a period of 5–15 μsec , parallel particle and energy transport to the wall was still possible. Also, the parallel field path for the axial current along the outside of the separatrix was blocked during that time, forcing partial commutation of the current through the X points into the center of the toroid.

However, with this coil setup, it was possible to create very oblate toroids with $L/R \sim 1$. These toroids were susceptible to a combined shift and tilt. In fact, the signals from the magnetic probes were very difficult to interpret in these cases, since both the shift and the tilt did not always occur in

the same plane, and only occasionally in the plane of the probe array.

Approximately spherical toroids were stable for low field reversal as long as the separatrix still enclosed the bias coil in the midplane. After the current in this coil had been reversed, some shifting of the toroid was observed. However, as soon as the shift developed sufficient amplitude, such that the separatrix came close to the bias coil, the resulting restoring force limited the instability. Field-reversal times of up to 40 μsec were obtained, but during the first 10–15 μsec , the separatrix stayed outside the wall in the midplane. The L/R ratio of the best behaved cases was about one. Considerable open axial current passed through the center of the toroid.

The Thomson-scattering diagnostic gave peak electron temperatures of about 10 eV for a fill density of $2 \times 10^{15} \text{ cm}^{-3}$ (Fig. 6). Reducing this density by a factor of three increased the peak temperature slightly to 15 eV; further reduction gave no improvement. Relative density measurements by the same diagnostics showed a reduction in density at the time of peak temperature according to the change in fill density between 2×10^{15} and $7 \times 10^{14} \text{ cm}^{-3}$; a further decrease in fill density to $1 \times 10^{14} \text{ cm}^{-3}$ resulted in a constant measured density or even a slight increase. This may be due to a base impurity level which is independent of the fill, as well as to a change in the dynamics of the plasma. After formation, temperatures soon decrease to 5–8 eV in all cases. As may be expected by the reduced Alfvén time at low densities, macroscopic unstable decay takes place much more easily. Also, there is an enhanced diffusion of magnetic field.

V. EXPERIMENTS WITH ADDITIONAL STABILIZATION

The studies presented in the preceding paragraphs demonstrated that the stability of the toroid is strongly influenced by its shape, in agreement with theoretical predictions. Although stability was observed for the plasma lifetime in one particular case, in general, the toroid eventually becomes unstable in a long-lasting external field which does not match the internal-field decay rate. In larger experiments, however, matching the applied-field decay rate to the internal decay rate is impractical, since one would tend to use dc fields for the external magnetic configuration.

In the PS-1 experiment, other means of stabilizing the toroid were investigated. As was mentioned, wall stabilization is expected to be very effective, provided the distance from the wall to the separatrix, measured by the ratio of the wall to separatrix radius (r_w/r_s), is not too large.^{3,13} Since the formation scheme of the PS-1 experiment is not compatible with flux-conserving walls, a thin metallic liner was inserted [Fig. 1(e)] along the azimuthal wall of the device. It consisted of a 50 μm stainless steel sheath having an L/R time of about 5 μsec . Thus, the rise time of the reversal field as seen from the plasma was slightly slower than before, and the peak amplitude was reduced.

With this arrangement, it was possible to stabilize the toroid for about 10–15 μsec in cases which were unstable without a liner (Fig. 7). After this time, the radius of the toroid had shrunk ($r_w/r_s = 1.6$), and a slight radial shift was

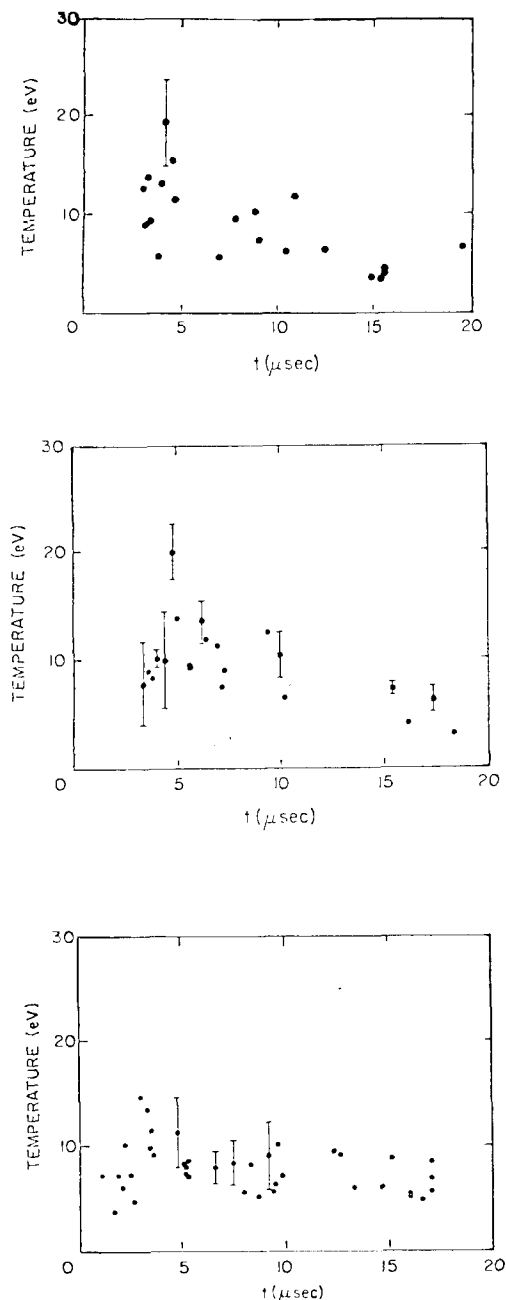


FIG. 6. Electron temperatures for coil configuration 1(d). The fill densities are 2, 7, and $20 \times 10^{14} \text{ cm}^{-3}$, respectively.

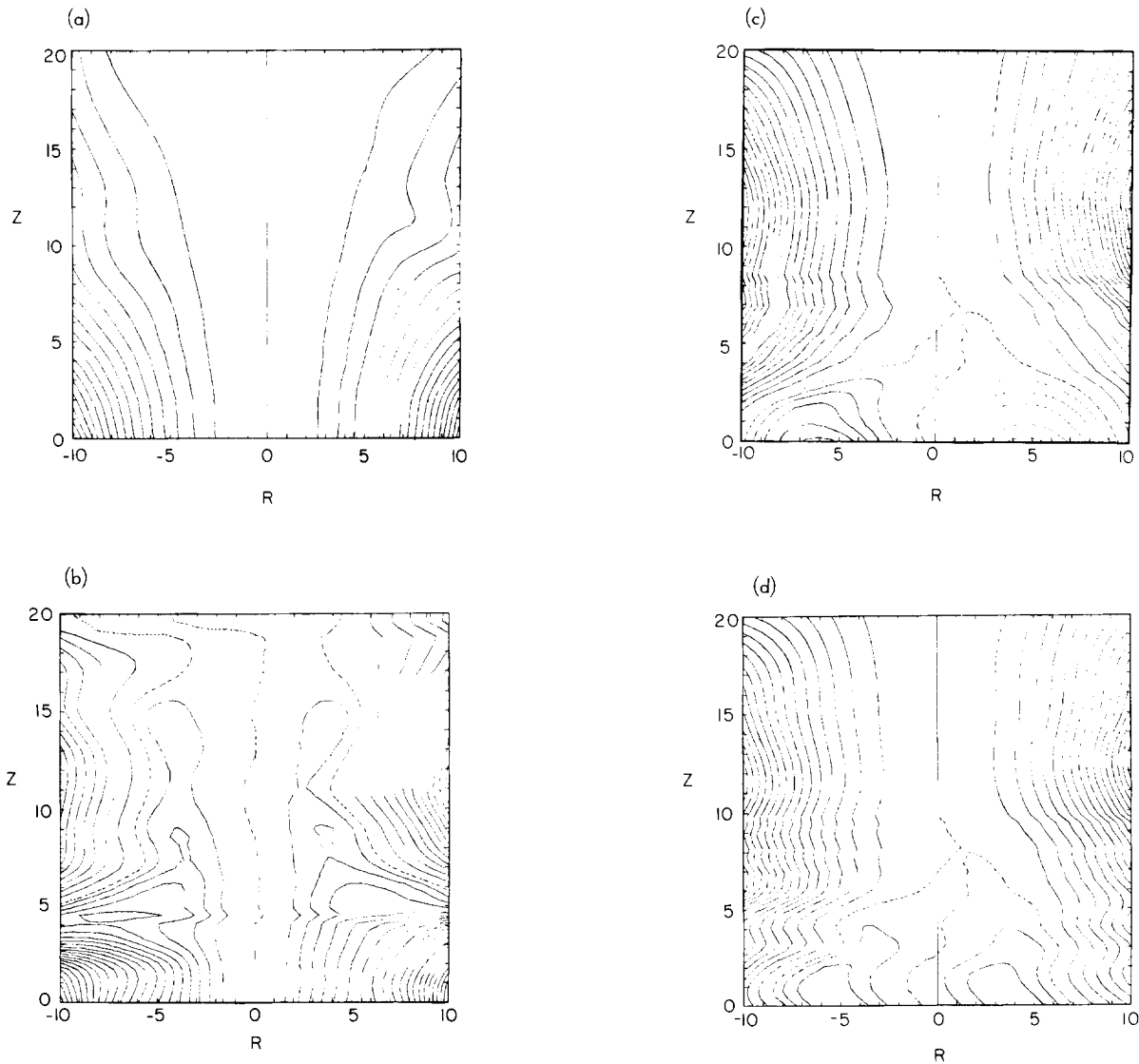


FIG. 7. Contours of constant poloidal flux at different times for coil configuration 1(d). Inside the separatrix (dashed line) the flux increment is $2\pi \times 5 \text{ kG cm}^2$, outside the increment is $2\pi \times 10 \text{ kG cm}^2$. (a) $t = 0$ (start of reversal), (b) $t = 4 \mu\text{sec}$, (c) $t = 8 \mu\text{sec}$, and (d) $t = 15 \mu\text{sec}$. A radial shift is noticeable by the oscillations of the contours, stemming from discharge-to-discharge variation in the direction and speed of the shift.

observed [Fig. 8(a)].

Besides suppressing the tilt stability, the liner reduced the amount of open axial current passing through the separatrix-bounded region. In previous cases, the current commuted back along the poloidal field lines, crossing the X points (through the center of the toroid). This was because the current path along the outside of the separatrix was blocked during the formation by the separatrix intersecting the dielectric walls. Now, in the same time interval, the external current is directed to the liner and continues to flow along this metallic path.

Another positive effect of the liner is to reduce the influx of impurities from the walls. An additional large reduction in the C III line intensities took place after we removed the glass envelopes from the rear of the elkonite electrodes and established a continuous rf discharge in 0.1 mTorr hydrogen between shots.

The use of Ioffe currents as an additional method of stabilization was tested. Theoretically, the effect of these currents on a spheromak is ambiguous. While for simple mirror geometry the stabilizing influence is well documented, the additional poloidal-field reversal and the toroidal-field component may lead to a destabilization of other modes in the spheromak.

The experiment was performed with both a dodecapole and a hexapole arrangement. The current per rod was varied in both cases from 10–35 kA. There was little difference between the two configurations; the dodecapole was, however, slightly more effective. Generally, a reduction of the radial shifting speed was found, but a completely stable toroid could be obtained only occasionally. The shift was found to develop at random in both speed and direction.

To reduce the oblateness of the toroid, the antimirror ratio of the bias field was decreased by moving the bias coils

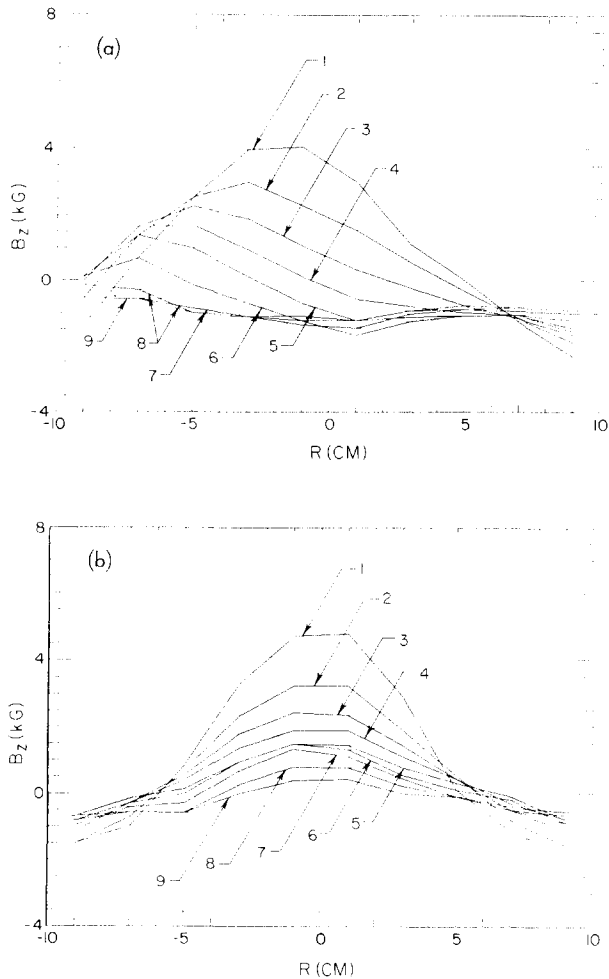


FIG. 8. Radial profiles of axial magnetic field in the midplane at several times for (a) coil configuration 1(e) with liner and (b) with the addition of the "figure-eight" stabilization coils. The peak value of the magnetic field corresponds to the symmetry axis which drifts radially in (a) but not in (b). The numbers 1–9 refer to time from 27.5 to 47.5 μsec in steps of 2.5 μsec .

from the midplane to axial positions of ± 5 cm [Fig. 1(e)]. In addition, a third center coil for the reversal field was installed [Fig. 1(f)]. This coil had a 25% higher inductance than the outer ones. With this arrangement, it was possible to obtain the longest field-reversal times (40 μsec , as measured from the time the separatrix is fully inside the chamber). Application of Ioffe currents resulted in a reduction of the lifetime by 5 to 10 μsec .

Figure 5(b) shows the measured magnetic energy W , helicity K , and the eigenvalue $k = W/K$ for case 1(e) (i.e., without Ioffe currents and the reversal-field center coil). An estimate of the eigenvalue k can be made from the measured radius r and length l of the separatrix: for a cylindrical model, $k^2 = (\pi/l)^2 + (3.8/r)^2$; for a spherical one, $k = 4.49/r$. At times where the separatrix is fully in the area covered by magnetic-probe measurements and appears spherical, the latter eigenvalue corresponds reasonably well to the measured one.

Recently, Jardin and Christensen²¹ proposed the use of "figure-eight" coils to stabilize the tilt and shift modes. While the tilt mode in PS-1 had been well controlled by appropriate shaping of the toroid in the presence of the metallic

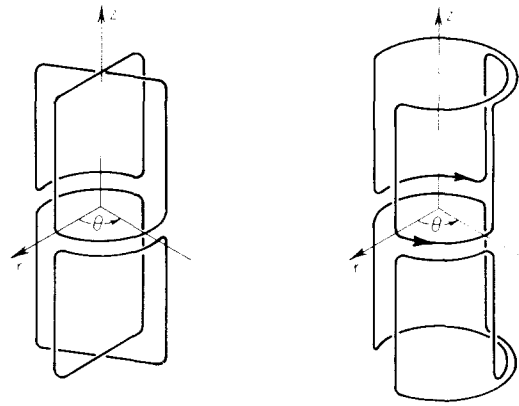


FIG. 9. Two different types of coils used to stabilize the $n = 1$ motion. For each type only two of four coils are shown.

liner, the shift was stabilized completely by a set of these passive coils (Fig. 8). In the experiments performed so far, these coils span the entire toroid, reaching from both axial ends ($z = 20$ cm) along the liner to the midplane (Fig. 9). Studies are now in progress to find the optimum shape and minimum area of these coils necessary for stability.

VI. CONCLUSIONS

For many years, interest in minimum magnetic energy, force-free configurations had been restricted to theoretical investigations. Recently, experiments in the PS-1 device, together with experiments using magnetized guns,⁵ the slow-induction scheme,⁷ and conical theta pinches,⁶ have demonstrated that a variety of methods exist for the production of spheromak plasmas. In particular, the technique discussed here provides an easy means of forming a toroid and confining it in an external guiding field. It is an extremely versatile method, since both the mirror ratios of the bias and reversal fields, the amplitude of the axial current, as well as the temporal programming can be varied easily.

In the experiments reported here, it has been shown that formation on the timescale of a few Alfvén times and also on a slower timescale is possible. These experiments demonstrate the feasibility of applying this formation scheme in larger devices, which will require slow timescales.

Extensive studies on shaping the toroid showed that theoretical expectations of the tilt and shift instability agree with experimental results. The quantitative agreement of the experiment with force-free models (or in the case of nonnegligible plasma pressure "nearly force-free" models) is remarkable when one notes that the configuration is not identical to the theoretical models and differs in the shape of the external equilibrium field. Optimization of the toroid shape and the application of a thin liner and "figure-eight" coils stabilized the toroid against tilt and shift modes for the timescale of the applied field.

Although radiation by impurities is not the major loss channel during formation, the lifetime of the field-reversed state seems to be limited by this mechanism. A considerable reduction in carbon line radiation has been achieved by introducing the metallic liner, eliminating all dielectric material from the neighborhood of the plasma, and employing con-

tinuous-rf-discharge cleaning between the shot. This, however, is not sufficient to overcome the radiation barrier. A further reduction of the impurity level, which is estimated to be 2%–4% carbon and oxygen, is required.

At the standard fill density of $2 \times 10^{15} \text{ cm}^{-3}$, maximum lifetimes in excess of 40 μsec for well-confined toroids have been measured. This time of field reversal is consistent with the measured electron temperatures of 5–8 eV at late times and a nearly classical magnetic-field diffusion. Ion temperatures at early times in excess of electron temperatures indicate anomalous ion heating during formation.

ACKNOWLEDGMENTS

We thank K. R. Diller, E. Day, and D. Miller for their technical support during the construction and operation phases of the experiment.

This work was supported by the U.S. Department of Energy. H. B. was supported by the Humboldt Foundation.

- ¹J. B. Taylor, in *Proceedings of the 5th International Conference on Plasma Physics and Controlled Nuclear Fusion Research*, Tokyo, 1974 (IAEA, Vienna, 1975, Vol. I, p. 161); J. B. Taylor, *Phys. Rev. Lett.* **33**, 1139 (1974); J. B. Taylor, in *Pulsed High Beta Plasmas* (Pergamon, Oxford, 1976), p. 59.
- ²S. Chandrasekhar and L. Woltjer, *Proc. Natl. Acad. Sci. USA* **44**, 285 (1958); L. Woltjer, *ibid.* **44**, 489 (1958); L. Woltjer, *ibid.* **44**, 833 (1958); L. Woltjer, *ibid.* **45**, 769 (1959); D. R. Wells, *Phys. Fluids* **5**, 1016 (1962); *ibid.* **7**, 826 (1964); *ibid.* **9**, 1010 (1966); G. K. Morikawa, *Phys. Fluids* **12**, 1648 (1969); G. K. Morikawa and E. Rebhan, *Phys. Fluids* **13**, 497 (1970); and Tyan Yeh and G. K. Morikawa, *ibid.* **14**, 781 (1971).
- ³H. A. Bodin and A. A. Newton, *Nucl. Fusion* **20**, 1255 (1980).
- ⁴M. N. Bussac, H. P. Furth, M. Okabayashi, M. N. Rosenbluth, and A. M. Todd, in *Proceedings of the 7th International Conference on Plasma Physics and Controlled Nuclear Fusion Research*, Innsbruck, 1978 (IAEA, Vienna, 1979), Vol. 3, p. 250; M. N. Rosenbluth and M. N. Bussac, *Nucl. Fusion* **19**, 489 (1979); Z. G. An, A. Bondeson, H. Bruhns, H. H. Chen, Y.

- P. Chong, J. M. Finn, G. C. Goldenbaum, H. R. Griem, G. W. Hart, R. Hess, J. H. Irby, Y. C. Lee, C. S. Liu, W. M. Manheimer, G. Marklin, and E. Ott, in *Proceedings of the 8th International Conference on Plasma Physics and Controlled Nuclear Fusion Research*, Brussels, 1980 (IAEA, Vienna, 1981), Vol. 1, p. 493.
- ⁵E. H. A. Gruneman, G. C. Goldenbaum, J. H. Hammer, C. W. Hartman, D. S. Prono, J. Taska, and W. C. Turner, in *Proceedings of the 10th European Conference on Controlled Fusion and Plasma Physics*, Moscow, USSR, September 1981 (to be published); Lawrence Livermore National Laboratory Preprint. No. UCRL 85912, 1981.
- ⁶E. E. Nolting, P. E. Jindra, and D. R. Wells, *J. Plasma Phys.* **9**, 1 (1973).
- ⁷M. Yamada, H. P. Furth, W. Hsu, A. Janos, S. Jardin, M. Okabayashi, J. Sinnis, T. H. Stix, and K. Yamazatzi, *Phys. Rev. Lett.* **46**, 188 (1981).
- ⁸G. C. Goldenbaum, J. H. Irby, Y. P. Chong, and G. W. Hart, in *Proceedings of the 9th European Conference Controlled Fusion and Plasma Physics*, Oxford, 1979 (Culham, Abingdon, 1979), p. 129; G. C. Goldenbaum, J. H. Irby, Y. P. Chong, and G. W. Hart, *Phys. Rev. Lett.* **44**, 393 (1980).
- ⁹S. C. Jardin, and W. Park, *Phys. Fluids* **24**, 679 (1981); J. M. Finn, W. M. Manheimer, and E. Ott, *Phys. Fluids* **24**, 1336 (1981).
- ¹⁰W. T. Armstrong, R. K. Linford, J. Lipson, D. A. Platts, and E. G. Sherwood, *Phys. Fluids* **24**, 2068 (1981).
- ¹¹T. R. Jarboe, I. Henins, H. W. Hoida, J. Marshall, and A. R. Sherwood, in *Proceedings of the US-Japan Joint Symposium on Compact Toruses and Energetic Particle Injection*, December 1979 (PPPL, Princeton, 1980), p. 53.
- ¹²H. Bruhns, Y. P. Chong, G. Goldenbaum, G. Hart, and R. A. Hess, in *Proceedings of the Third Symposium on the Physics and Technology of Compact Toroids in the Magnetic Fusion Energy Program*, Los Alamos, New Mexico, December 1980, Los Alamos National Laboratory Report No. LA-8700-C, 1981.
- ¹³J. M. Finn and A. Reiman, *Phys. Fluids* **25**, 116 (1982).
- ¹⁴G. Miley, in Ref. 11, p. 200; M. Katsurai and M. Yamada, in Ref. 11, p. 212.
- ¹⁵A. G. Sgro and D. Winske, *Phys. Fluids* **24**, 1156 (1981).
- ¹⁶S. C. Jardin, M. S. Chance, R. L. Dewar, R. C. Grimm, and D. A. Monticello, *Nucl. Fusion* **21**, 1203 (1981).
- ¹⁷H. Alfvén and L. Lindberg, *Moon* **10**, 323 (1974).
- ¹⁸H. Alfvén, L. Lindberg, and P. Mitlid, *J. Nucl. Energy C1*, 116 (1960).
- ¹⁹J. H. Irby, J. H. Drake, and H. R. Griem, *Phys. Rev. Lett.* **42**, 228 (1979).
- ²⁰A. Reiman, *Phys. Fluids* **25**, 1885 (1982).
- ²¹S. Jardin and U. R. Christensen, *Nucl. Fusion* **21**, 1665 (1981).